DEVELOPMENT OF FRAGILITY CURVES FOR SOIL EMBANKMENT SLOPES DUE TO FUTURE EXTREME RAINFALL EVENTS

Leila Baninajarian, & Rashid Bashir
Department of Civil Engineering - York University, Toronto, Ontario, Canada
Ali Ghassemi
GHD, Mississauga, Ontario, Canada
Andrew DeSira & Tony Sangiuliano
Ministry of Transportation of Ontario, Toronto, Ontario, Canada

ABSTRACT
The performance of earth embankments is essential in sustaining the transportation infrastructure. Increasing the likelihood of extreme precipitation as a consequence of climate change can create embankment failures. The objective of this paper is to develop fragility curves for earth embankments under extreme rainfall events in Niagara Falls. For this purpose, a series of reliability analyses were carried out to consider the effects of soil parameter uncertainties on the stability of the embankment slopes under various extreme rainfall events. The developed fragility curves for sand embankments show a decreasing trend in the probability of failure with an increase in return period and rainfall duration.
Contrary to sand embankments, the developed fragility curves for silt embankment generally show an increasing trend in the probability of failure with increasing rainfall return period. It can also be observed that the probability of failure for silt embankment is higher for future conditions in comparison to the historical conditions. Besides, the occurrence of a shallow failure in this type of embankment is more probable than general failure.

RÉSUMÉ
La performance des remblais en terre est essentielle au maintien des infrastructures de transport. L'augmentation de la probabilité d'une participation extrême en raison du changement climatique peut créer des défaillances de remblai. L'objectif de cet article est de développer des courbes de fragilité pour les remblais de terre sous des événements de précipitations extrêmes à Niagara Falls. À cette fin, une série d'analyses de fiabilité ont été effectuées pour examiner les effets des incertitudes des paramètres du sol sur la stabilité des talus de remblai sous divers événements de précipitations extrêmes. Les courbes de fragilité développées pour les remblais de sable montrent une tendance à la baisse de la probabilité d'échec avec une augmentation de la période de retour et de la durée des précipitations. Contrairement aux remblais de sable, les courbes de fragilité développées pour les remblais de limon montrent généralement une tendance à la hausse de la probabilité de défaillance avec l'augmentation de la période de retour des précipitations. On peut également observer que la probabilité de défaillance du remblai de limon est plus élevée pour les conditions futures par rapport aux conditions historiques. De plus, la survenue d'une défaillance superficielle dans ce type de remblai est plus probable qu'une défaillance générale.

1 INTRODUCTION

1.1 The Vulnerability of Soil Embankments to Climate Change

The Intergovernmental Panel on Climate Change has reported that the climate change process would continue over the next century (IPCC 2013). Changes in many extreme kinds of weather and climate events, including an increase in the number of extreme precipitation events in several regions have been observed since, about 1950 (IPCC 2015). Highway embankments are required to be operational over their lifetime and are likely to experience rainfall-induced slope failures because of their continuous exposure to changing atmospheric conditions.

A considerable amount of water exchanges takes place at the soil-atmosphere boundary. Prevailing atmospheric conditions at the ground surface can change the water storage in the slope. Increased water storage causes increase the pore water pressure and decrease the suction component of the shear strength. These changes in pore pressure and shear strength can lead to slope instabilities (Fredlund et al. 2012). The stability of slopes is usually expressed in terms of the factor of safety (FOS). The factor of safety against slope failure is a single value index. The slope is considered as “safe” if the calculated FOS is higher

than the reference value (e.g., 1.0) or “unsafe” otherwise. There are inevitable uncertainties in various factors influencing the stability of slopes. These uncertainties may lead to uncertainty in the factor of safety that is not considered in the conventional slope stability analyses.

Uncertainties in rainfall characteristics, along with uncertainties in soil strength and soil hydraulic properties are the most important source of uncertainties, influencing the stability of embankment slopes exposed to the environment. Fragility curves in reliability analyses offer an opportunity to evaluate these uncertainties and estimate their effects on the slope stability using probabilistic concepts. This study is a part of a research project on the effects of climate change on the stability of highway embankments across Ontario. In this paper, the probability of instability in soil embankments due to historical and future extreme rainfalls in the city of Niagara Falls is investigated.

1.2 Background

Fragility curves are developed when the probability of failure for various possible loading conditions needs to be evaluated in slope stability analyses. Fragility curves relate the probability of failure (P_f) with the intensity of the applied loads and are an appropriate tool for reliability-based analysis of slope stability. The advantages of the developing fragility curves include the allowance for an explicit appraisal of the uncertainties associated with vulnerability modeling and the possibility of presenting results for a wide range of loadings. This makes fragility curves an attractive tool for carrying out risk assessments of large systems, such as major transport networks (Martinović et al. 2018). To date, the most research on vulnerability assessment of slopes has focused on slope performance under earthquake loading (e.g., Fotopoulou and Pitilakis, 2013) and only a few researchers have presented fragility curves for slope stability under extreme rainfall events (Otálvaro and Cordao-Neto 2013; Jasim et al. 2017; Martinović et al. 2018)

It is important to mention that fragility curves are basically established to show the probability of failure for all feasible loads (herein rainfall), and the probability of load exceedance is not taken into account explicitly. Hence, the probability of failure given by fragility curves is indeed the conditional probability of failure. This issue is fundamental to be addressed in the development of fragility curves. However, most of the previous studies have focused on rainfall intensity and duration without taking into consideration the probability of event occurrence. For example, Martinović et al. (2018) numerically studied the probability of rainfall-induced slope failure and developed fragility curves using duration as the primary independent variable. Although the conditional probability of failure under different rainfall conditions was addressed by developing a set of fragility curves, the probability of rainfall reoccurrence was ignored in their study.

The probability of the event reoccurrence can be incorporated into the fragility curve concept by developing the curves for different return periods. For example, Jasim et al. (2017) developed fragility curves for a case study, considering different rainfall scenarios, including rainfall durations of 1 to 7 days and recurrence intervals of 25, 50, and 100 years. In the developed fragility curve, the rainfall intensity was set as the primary independent variable for fragility curves. Although such fragility curves have the advantage of including rainfall return period, the occurrence of rainfalls with more than 1-day duration with uniform intensity is rare.

2 DEVELOPMENT OF FRAGILITY CURVES FOR SOIL EMBANKMENT UNDER EXTREME RAINFALL

2.1 Geometry and Material

The embankment profile considered in the current study represents a typical highway embankment in Ontario, as shown in Figure 1.

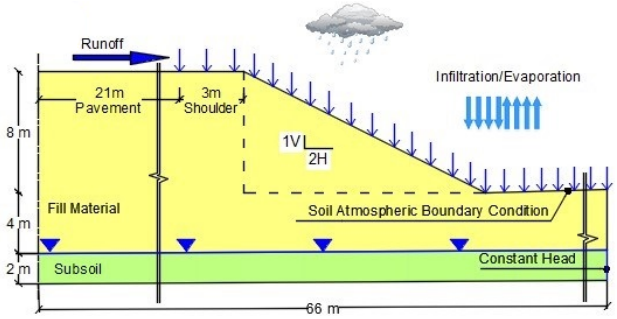

Figure 1. Typical highway embankment in Ontario considered in this study

The fragility curves were developed for sandy silt and silty sand materials, from now on named sand and silt, respectively, which are typically used in the construction of highway embankments in Ontario. The saturated unit weight of 20.7 kN/m^3 and 19 kN/m^3 was considered for sand and silt, respectively. Moreover, the specific gravity (Gs) of 2.65 for sand and 2.67 for silt were assumed in this study.wThe soil-water characteristic curves (SWCC) for these materials are shown in Figure 2.

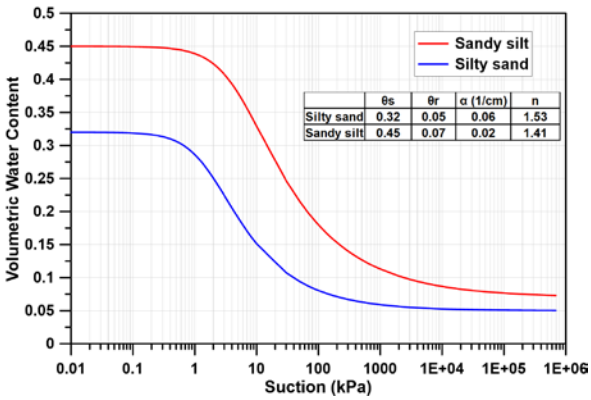

Figure 2. SWCC for typical embankment materials

The van Genuchten (1980) function was used to describe the SWCC.

$$Se = \frac{\theta(\psi) - \theta r}{\theta s - \theta r} = (1 + |\alpha\, \psi|^{n})^{-m} \quad [1]$$

Unsaturated hydraulic conductivity functions (HCF) for these materials were determined from SWCC using the van Genuchten-Mualem approach (Mualem 1976, van Genuchten 1980).

$$K(\psi) = Ks(Se)^{l}\left\{\left[1 - \left[1 - (Se)^{l/m}\right]^{m}\right]\right\}^{2} \quad [2]$$

In Equations 1 and 2, K_s is the saturated hydraulic conductivity, S_e is the effective water saturation ($0< S_e <1$), θ_s is the saturated volumetric water content, θ_r is the residual volumetric water content, and , n, and m are empirical parameters that depend on the soil type and can be estimated by fitting Equation (1) to the measured SWCC data. The parameter m is commonly assumed to be equal to $1 - 1/n$ (van Genuchten 1980). In Equation 2, l is the pore interaction factor and its value has been found to be 0.5 for a wide variety of soils (Mualem 1976).

2.2 Methodology

In this study, fragility curves were developed for a typical embankment, as shown in Figure 1, under various historical and future rainfalls. For this purpose, a 30-year historical climate dataset (i.e., 1981-2010) and sixteen 90-year (i.e., 2011-2100) future climate datasets were compiled, classified, and analyzed for the city of Niagara Falls. Long-term variation of soil moisture conditions under different future climate scenarios was investigated using 1D transient unsaturated seepage finite-element (FE) simulations to identify an appropriate long term design climate that could produce critical conditions in the soil embankment. These conditions could cause the lowest possible factor of safety against slope failure in the soil embankment. The factor of safety is a function of pore pressure distribution within the embankment and is directly affected by the climate. A wetter climate, in general, can create higher pore water pressure distributions, which can result in a lower FOS. Therefore, the design climate should contain a probable wettest condition.

In order to compare the long-term effects of different future climate scenarios on two soil types, the frequency of high saturation occurrence (number of events that saturation degree of the soil exceeds the maximum saturation degree experienced during the historical period) were considered. As shown in Figure 3, the future climate data based on the GCM GFDL and RCP 2.6 would cause the highest values of saturation in both sand and silt embankments. It can also be observed that for the same scenario, the number of events when this saturation occurs is also very high. Therefore, this scenario was chosen as the critical scenario for Niagara Falls.

Long-term variations of the spatial distribution of pore water pressure (PWP) within the embankments were obtained using 2D transient unsaturated seepage finite-element (FE) models under the selected climate scenario. Assessment of slope stability overtime during extreme precipitation events was carried out by exporting PWP spatial distributions based on the 50% percentile of daily soil saturation data obtained from long-term HYDRUS 2D analyses into a 2D limit equilibrium slope stability model. The 50% percentile was considered to be the most probable initial moisture condition in the slope at the time of occurrence of an extreme event.

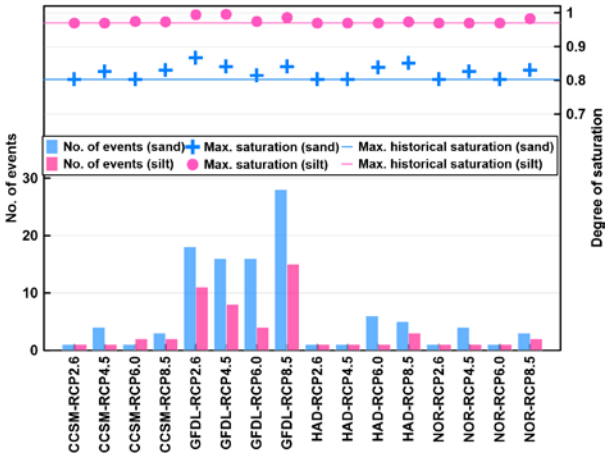

Figure 3. Maximum saturation degree and frequency of high saturation occurrence in sand and silt material for Niagara Falls

In order to select the future extreme rainfall scenario for slope stability assessment under extreme rainfall, historical IDF curves based on 30 years of historical climate data (i.e., 1981-2010), were obtained from Environment Canada. These were considered as the datum. Future IDF curves, available from the Ministry of Transportation, Ontario (MTO 2018), and the Ontario Climate Change Data Portal (CCDP 2018), were compiled and analyzed. The IDF curves by MTO have been developed using time trend analysis with observations from 1960 to 2014. However, the future IDF curves by CCDP are predicted using two different regional climate models, namely PRECIS and RegCM. The IDF curves are available for emission scenarios A1B, RCP4.5, and RCP8.5 based on both fourth (AR4) and fifth Assessment Report (AR5) of the IPCC. Both MTO and CCDP future IDF curves show a significant increase in future extreme precipitation during the last 30 years of this century (i.e., 2070-2100). Predicted IDF curves for this period were considered in the current study. The future IDF curves for three different return periods from CCDP and MTO for the city of Niagara Falls are shown in Figure 4.

A review of this figure indicates that for all return periods, CCDP`s IDF curves predict higher intensities for longer durations compared to MTO. Among all IDF curves by CCDP, IDF curves for scenarios A1B-P90% (A1B scenario with 90 percentile) and RCP8.5-RegCM show

higher predictions of the rainfall intensities. Since A1B-P90% is part of the older assessment report of IPCC, IDF curves from RegCM under RCP8.5 were taken as the critical scenario in this study. Figure 5 shows the percent change in intensity of 1, 6, and 24-hour extreme rainfall under the selected scenario for various returns periods in Niagara falls. It can be observed that the change of 24-hour rainfall with the 100-year return period in the future is greater than the other cases.

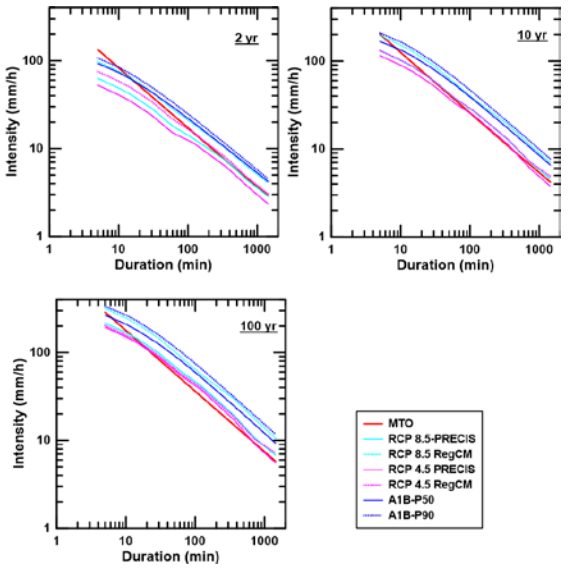

Figure 4. Comparison between different future IDF curves

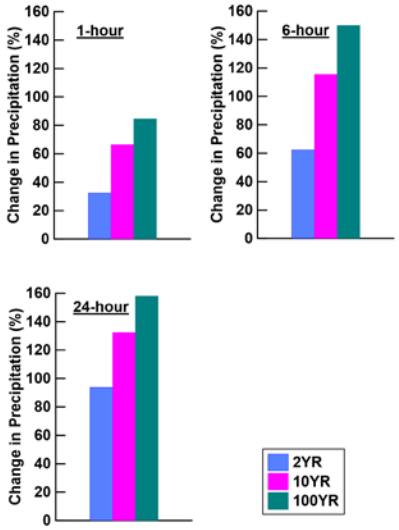

Figure 5. Change in intensity of 1,6, and 24-hour precipitation events for various returns periods in Niagara Falls

In the next step, the coupled hydro-geotechnical modules of a software suite called GeoStudio (Geo-slope International Ltd. 2016) were used to investigate the embankment stability under historical and future design storms. The factor of safety (FOS) against slope failure was considered as the primary indicator of slope stability conditions. In this research, two types of failure, general and shallow failures were investigated. Since a minimum sliding mass depth should be defined in the limit equilibrium analyses to consider the depth of failure surface, a minimum slip depth of 1.0 m and 0.3 m were assigned for general failures and shallow failures, respectively. The soil-atmosphere boundary for the hydrological model was prepared using Chicago storm hyetographs based on historical and selected future intensity-duration-frequency (IDF) curves. The method proposed by Keifer and Chu (1957), known as the Chicago design storm, was used in this study. This method has been widely used in Canadian practice (Marsalek and Watt, 1984). The method also has been suggested by MTO to be applied for assessment of the storm impacts to the drainage systems (MTO 1997).

Finally, the probabilistic analyses were employed to estimate the probability of slope failure based on the critical FOS, which is the minimum factor of safety throughout an extreme event, obtained from slope stability analyses, and develop the fragility curves under different rainfall scenarios. Instead of using intensity or duration, the return period, which is a standard and important tool in hydrological engineering design, was considered as the primary independent variable for the fragility curves.

2.3 Probabilistic analysis

Mathematically, the FOS can be considered as a function of all factors influencing it. Therefore, the uncertainties in the influencing factors lead to uncertainty in FOS. The main object of reliability analysis is to estimate the probability distribution of FOS. In this regard, it is common to define the performance function *G(X)* that relates to FOS as following:

$$G(X) = FOS(X) - 1 \quad [3]$$

Where $X = (x_1, x_2, \dots, x_N)$ is a vector of the *N* random variables x_i representing various influencing parameters, which in this study are soil parameters affecting the slope stability. For each x_i, a distribution function is assumed, but the joint distribution of vector *X* is unknown. As mentioned before, safety in the context of a probabilistic analysis is typically expressed in terms of a probability of failure (P_f) and reliability index *(β):*

$$P_f = P[G(X) \leq 0] \quad [4]$$

$$\beta = E[G(X)]/\sigma[G(X)] \quad [5]$$

Where $E[G(X)]$ and $\sigma[G(X)]$ are the mean and standard deviation of the performance function, respectively. The definition of P_f and β are illustrated in Figure 6. P_f indicates the probability of slope failure (the area under the probability distribution of *G(X)≤0*), while β

represents the mean of performance function in terms of its standard deviation. A higher mean value of FOS and/or lower standard deviation of its distribution would result in a higher reliability index. It should be noted that the above definition is accurate if the performance function (or factor of safety equation) is linear, which is not the case for slope analysis models (El-Ramly et al. 2002). Mostyn and Li (1993) suggested, however, that the performance functions of slopes are reasonably linear and recommended ignoring the nonlinearity when calculating *β*.

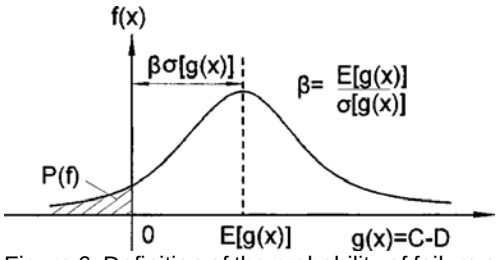

Figure 6. Definition of the probability of failure and reliability index on a normal distribution curve (Xue and Gavin 2007)

In this study, the first-order second-moment method (FOSM) was used to estimate the reliability analysis. This method is based on Taylor's series expansion of the performance function around the mean vector of variables, and only first-order terms of the series are taken into account. If the input variables are not correlated, it can be shown that the mean and the variance of the performance function are given by the following equations:

$$E[G(X)] \approx G[E(x_1), E(x_2), \dots, E(x_N)] \quad [6]$$

$$\sigma^2[G(X)] \approx \sum_1^N (\frac{\partial G}{\partial x_i})\sigma^2[x_i] \quad [7]$$

If a probability distribution function is assumed for the performance function, its mean and standard deviation (Equations 6 and 7) can be used to calculate the probability for any of its values. If input variables are not independent, the correlation has to be taken into account for the calculation of the variance. The assumption of the probability distribution function for the performance function is one of the limitations of the FOSM method. Also, the first-order partial derivatives in Equation 7 must be numerically estimated using a finite difference scheme. A common practice is to select two points over a range of plus and minus one standard deviation with respect to the mean value of the random variable x_i, in order to capture the nonlinear behavior of the function in a range of likely values (Wolff 1994). Therefore, assuming *N* random variables, the number of simulations required to apply the FOSM method is *1+2N*. It is worth mentioning that using Monte Carlo simulation (MCS), which is a technique that often used to simulate the probability density function of a performance function, requires a large number of simulations, which is not practical for problems with small probabilities of failure and a large number of random variables.

Moreover, the application of the Taylor Series method in geotechnical engineering has been described elsewhere (e.g., Baecher and Christian 2005). It is common to use the following simple formula which was derived from Taylor series technique to estimate the standard deviation of the factor of safety (Wolff 1994; US Army Corps of Engineers 1997; Duncan 2000; Baecher and Christian 2005):

$$\sigma = \sqrt{(\frac{\Delta FOS_1}{2})^2 + (\frac{\Delta FOS_2}{2})^2 + \cdots + (\frac{\Delta FOS_N}{2})^2} \quad [8]$$

Where $\Delta \mathrm{FOS_i} = (FOS_i^+ - FOS_i^-)$ and FOS_i^+ and FOS_i^- are the factor of safety calculated with the value of the $i\text{-}th$ parameter, respectively increased and decreased by one standard deviation from its mean value. In calculating FOS_i^+ and FOS_i^-, the values of all other parameters are kept at their mean values.

In this study, five soil hydraulic parameters (K_{sat}, α, n, θ_s and θ_r) and soil friction angle ***(φ)*** were considered as random variables. The mean value of these variables and their values considering standard deviation for sand and silt material, respectively, are presented in Tables 1a and b. Slope stability analyses were conducted under various historical and future rainfalls with six different return periods and three different durations to estimate the probability of failure in each case. As mentioned before, these analyses were done under the P50% initial conditions. The results were assimilated by developing a series of fragility curves, as described in the following section.

Table 1a. Sand parameters for reliability analysis

Parameters	Mean value	+ SD[1]	- SD
φ	34	36	32
K_{sat} [2] (m/hr)	0.0360	0.1671	0.0078
θs	0.32	0.38	0.25
θr	0.054	0.068	0.040
α (kPa)	1.750	1.294	2.701
n	1.53	1.71	1.34

Table 1b. Silt parameters for reliability analysis

Parameters	Mean value	+ SD[1]	- SD
φ	32	34	30
$Ksat$ (m/hr)	0.0045	0.021	0.001
θs	0.45	0.53	0.37
θr	0.067	0.081	0.053
α (kPa)	4.9	2.98	13.88
n	1.41	1.53	1.29

[1]SD: Standard deviation, [2] The log scale was used for K_{sat}.

3 RESULT AND DISCUSSION

Figures 7 a and b show the fragility curves for sand embankment under various historical and future rainfalls, corresponding to P50% initial moisture condition, and considering general and shallow failures, respectively. In addition to fragility curves, which show the variation of probability of failure with return period, the variation in the mean factor of safety (FOS) with return period is also presented in Figures 8 a and b.

For a variably saturated soil embankment under rainfall, the probability of failure is mostly governed by the uncertainties in the variation of soil shear strength, which is controlled by soil suction as well as soil shear strength parameters. The suction-related soil shear strength may increase or decrease with the increase in soil moisture. Therefore, the fragility curves may significantly differ in trend depending on the changes in moisture distribution during the rainfall. As presented in Figure 7, a decreasing trend in the probability of failure with increasing return period and duration of the event is observed for the minimum slip depth of 1m. This figure shows that sand embankment stability may not be affected by a 1-hour rainfall event. It seems logical as for shorter duration events such as 1-hour, only a small quantity of water can infiltrate into the embankment, and this quantity of water would not percolate deeper into the embankment.

For 30 cm slip depth, the changes in the probability of failure are different from those observed for 1 m slip depth. First, the probabilities of failure for shallower depths are, in general, higher than those observed for deeper depths. This is not surprising as climatic loads are known to have more effect on shallower depths (Pk et al. 2018). Secondly, for 1-hour storms, the probability of failure does not seem to be affected by the changing climate, which is similar to the results for 1m depth. However, for storms for 6 and 24-hour durations, there is a difference between probabilities of failure for historical and future extreme precipitation events. Results indicate that for future events, some increase in the probability of failure can be expected for 6 and 24-hour events. An increase in the probability of failure can also be observed for historical storms of returns periods greater than 10 years for 24-hour events. This observation is consistent with the increase in intensities and is indicative that these intensity increases are to the extent that they result in a reduction in the suction strength at shallower depths.

According to Figure 8 a and b, it can be seen that the mean FOS of slope changes only under future 24-hour rainfall in case of general failure. However, for shallow failure, both 6 and 24-hour rainfall can affect the FOS. It can also be seen that FOS decreases with an increase in average rainfall intensity either from lower to higher return periods or from historical to future events, although the minimum FOS corresponds to the future 100-year rainfall event is still above 1.25. The reason could be the influence of water content on soil suction strength. Under the small intensity of rainfall, the sand embankment is dry, and soil strength is low due to the small value of soil moisture content with P50% initial condition.

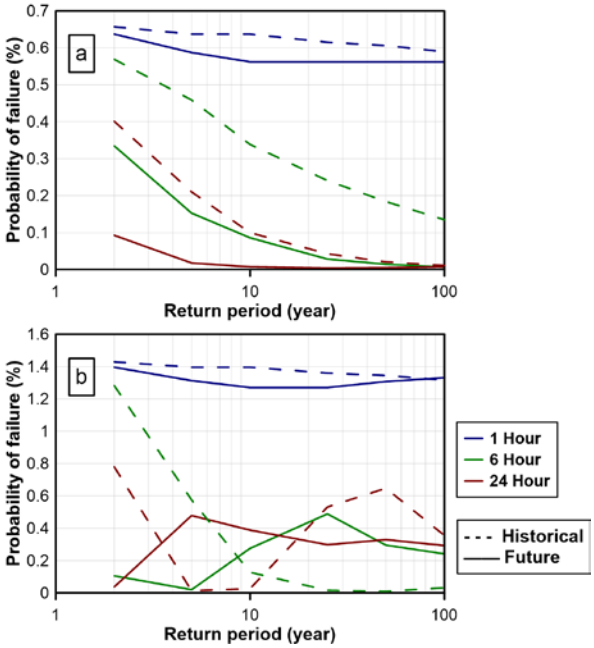

Figure 7. Fragility curves for sand embankment; a) General failure, b) Shallow failure

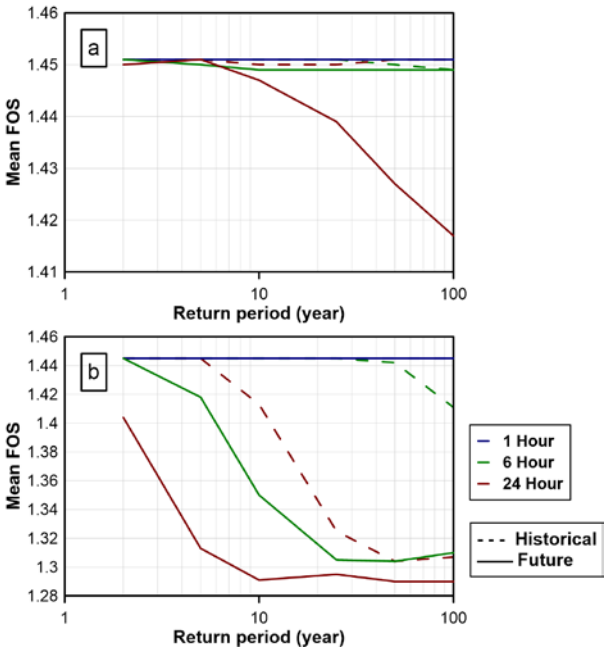

Figure 8. variation of the mean factor of safety over the return period in the sand embankment; a) General failure, b) Shallow failure

Figure 9 a and b show the fragility curves developed for silt embankment under various historical and future rainfalls corresponding to the P50% initial moisture conditions. The variation of the mean FOS is also presented in Figures 10 a and b. The first thing to notice is that the probabilities of failure are much larger for silt material as compared to sand material. This is consistent

with the previous studies that have shown that, in general, fine-grained materials are more prone to failure in comparison to coarse-grained materials (Pk et al. 2018). It can also be observed that shallower failures are more susceptible to historical and future climatic events, similar to the observations for the sand embankment.

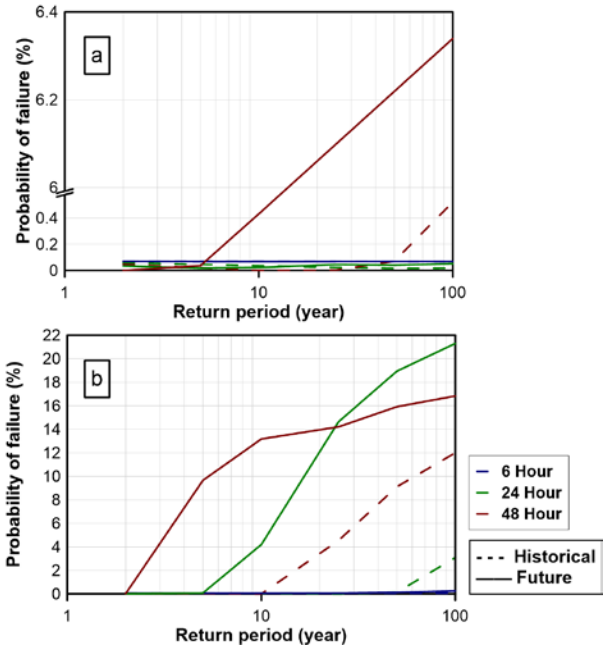

Figure 9. Fragility curves for silt embankment; a) General failure, b) Shallow failure

Contrary to the sand embankment, the developed fragility curves for silt embankment show a generally increasing trend in the probability of failure for both general and shallow failures with rainfall return periods. Additionally, more prolonged rainfall causes a considerable increase in the probability of failure. This observation is also consistent with results from others, where it has been reported that events of larger duration, result in more water entering the silt embankment owing to their lower intensities in comparison to shorter duration events and lower infiltration capacity of silt material (Pk et al. 2018). The main reason for the difference between the observations for embankments constructed with sand and silt materials can be attributed to the initial conditions. As shown in Figure 3, silt material tends to hold more water owing to its lower conduction and high retention properties in comparison to sand. Therefore, initial conditions for silt embankment are much higher than that for sand for the same percentile of occurrence. As a result, for similar storms, silt embankments could potentially end up at higher saturation than the sand embankment. This, coupled with the fact that silt material, in general, has a larger contribution from suction to its shear strength in comparison to sand (Lu and Likos 2006), is also responsible for higher probabilities of failure and larger increases due to climatic events. Accordingly, an increase in the probability of failure with increasing the return period (as rainfall intensity increases) along with a decrease in mean FOS for 24-hr and 48-hour rainfalls are observed in Figures 9 and 10 as a consequence of diminishing the positive role of suction in soil shear strength.

The abovementioned argument can also be extended to explain the differences between historical and future results. The substantial intensification of future rainfalls has an adverse effect on the safety of silt embankments in the future. For example, the probability of general failure under 48-hr, 100-year rainfall increases from less than 1% under historical to around 6% under future rainfall. Considering changes in mean FOS, it can also be seen that it changes from 1.6 in the historical period to 1.4 and 1.2 for general failure and shallow failure, respectively (Figure 10 a and b).

Comparing fragility curves for shallow failure and general failure indicates that the probability of shallow failure is much higher than general failure. Looking at fragility curves under 6-hour rainfall shows that the probability of failure increases from almost zero for general failure to 20% for shallow failure. It is according to the lower values of FOS for shallow failure compared to general failure as it can be seen in Figures 10 a and b that FOS under 48-hour 100-year return period changes from 1.4 in case of the general failure to 1.2 for shallow failure.

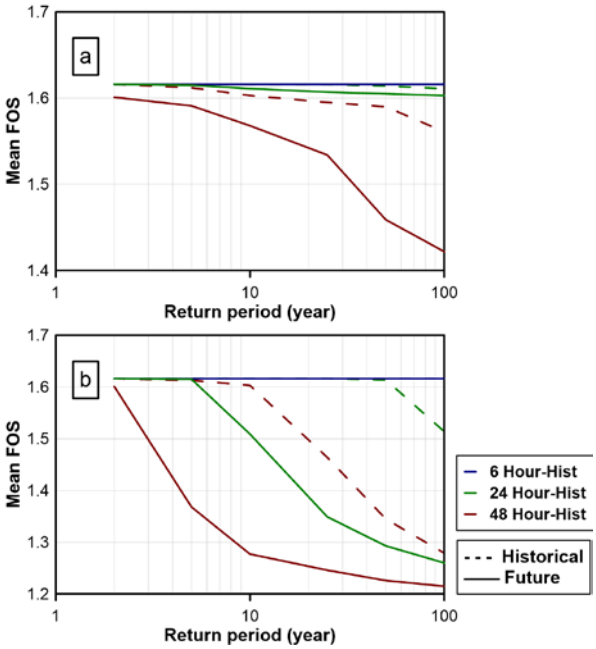

Figure 10. variation of the mean factor of safety over the return period in the silt embankment; a) General failure, b) Shallow failure

4 CONCLUDING REMARKS

In this study, the fragility curves for soil embankment slopes subjected to future extreme rainfall in Niagara Falls, Ontario, were developed. These fragility curves were developed for two different types of failure, general and shallow failures, corresponding to 1.0 and 0.3 m as

minimum depths of failure. The return period, which is a standard and important tool in hydrological engineering design, was considered as the primary independent variable for the fragility curve.

Evaluation of slope stability under extreme rainfall requires an accurate climate data analysis. Accordingly, in this study, the compilation, review, and analysis of the climate data have been done for the city of Niagara Falls, which suggests that the intensity of the future extreme precipitations events is expected to increase considerably for this city. This increase is expected for all durations and return periods. The increase in intensities is expected to be positively correlated with event duration and return period. Assessment of slope stability overtime during extreme events was carried out using a coupled hydro-geotechnical model. Then, fragility curves were developed using the results of the FOSM method as the reliability analyses considering various soil parameters as random variables. The developed fragility curves present the changes in slope stability with the return period of extreme rainfalls and examine how rainfall duration affects the slope stability under extreme rainfall events.

Overall, the results show that extreme rainfalls do not have a negative impact on the slope stability of sand embankment with P50% initial moisture conditions. However, embankments built with fine materials such as silt are susceptible to an increase in the probability of failures during prolonged rainfall events with a higher return period. The occurrence of a shallow failure in this type of embankment is more probable than general failure.

It must be noted that the estimated FOS is based on P50% initial condition, which provides the most probable initial moisture condition in the slope. Therefore, the given probability of failure in fragility curves is a conditional probability, and it can not reflect the total probability of failure within a given time frame. Accordingly, further study is proceeding to develop fragility curves under different initial conditions to see the effect of initial moisture condition on the stability of embankments under extreme rainfall.

5 REFERENCES

Baecher, G.B., and Christian, J.T. 2005. Reliability and Statistics in Geotechnical Engineering. John Wiley & Sons.

CCDP. 2018. CCDP - Ontario Climate Change Data Portal. Available from http://www.ontarioccdp.ca/.

Duncan, J.M. 2000. Factors of Safety and Reliability in Geotechnical Engineering. Journal of Geotechnical and Geoenvironmental Engineering, **126**(4): 307–316. American Society of Civil Engineers.

El-Ramly, H., Morgenstern, N.R., and Cruden, D.M. 2002. Probabilistic slope stability analysis for practice.

Fotopoulou, S.D., and Pitilakis, K.D. 2013. Fragility curves for reinforced concrete buildings to seismically triggered slow-moving slides. Soil Dynamics and Earthquake Engineering, **48**: 143–161. Elsevier.

Fredlund, D.G., Rahardjo, H., and Fredlund, M.D. 2012. Unsaturated Soil Mechanics in Engineering Practice.

van Genuchten, M.T. 1980. A Closed-form Equation for Predicting the Hydraulic Conductivity of Unsaturated Soils. Soil Science Society of America Journal, **44**(5): 892–898. Wiley.

Geo-slope International Ltd. 2016. Stability Modeling with SLOPE/W: An Engineering Methodology (Computer Program). GEOSLOPE/W International Ltd., Calgary, Alberta, Canada.

IPCC. 2013. Climate Change 2013. The Physical Science Basis Working Group I Contribution to the Fifth Assessment Report of the Intergovernmental Panel on Climate Change.

IPCC. 2015. Synthesis Report - Climate Change 2014.

Jasim, F.., Vahedifard, F., Ragno, E., AghaKouchak, A., and Ellithy, G. 2017. Effects of Climate Change on Fragility Curves of Earthen Levees Subjected to Extreme Precipitations Reusing Abandoned Natural Gas Storage Sites for Compressed Air Energy Storage View project Soil stabilization for road subgrade View project.

Keifer, C.J., and Chu, H.. 1957. Synthetic Storm Pattern for Drainage Design. Journal of the Hydraulics Division, **83**(4): 1–25.

Lu, N., and Likos, W.J. 2006. Suction Stress Characteristic Curve for Unsaturated Soil. Journal of Geotechnical and Geoenvironmental Engineering, **132**(2): 131–142. American Society of Civil Engineers.

Marsalek, J., and Watt, W.E. 1984. Design storms for urban drainage design. Canadian Journal of Civil Engineering, **11**(3): 574–584. NRC Research Press Ottawa, Canada .

Martinović, K., Reale, C., and Gavin, K. 2018. Fragility curves for rainfall-induced shallow landslides on transport networks. Canadian Geotechnical Journal, **55**(6): 852–861. Canadian Science Publishing.

Mostyn, G.., and Li, K.. 1993. Probabilistic slope analysis - State-of-play. *In* Conference on probabilistic methods in geotechnical engineering. A.A. Balkema, Rotterdam, Netherlands. pp. 89–109.

MTO. 1997. Drainage Management Manual. Ronin House Publishing, under contract from Ministry of Transportation of Ontario, Ottawa, Ontario, Canada.

MTO. 2018. IDF Curve Look-up - Ministry of Transportation. Available from http://www.mto.gov.on.ca/IDF_Curves/map_acquisition.shtml.

Mualem, Y. 1976. A new model for predicting the hydraulic conductivity of unsaturated porous media. Water Resources Research, **12**(3): 513–522. John Wiley & Sons, Ltd.

Otálvaro, I., and Cordao-Neto, M. 2013. Probabilistic analyses of slope stability under infiltration conditions.

Pk, S., Bashir, R., and Beddoe, R. 2018. Effect of Climate Change on Earthen Embankments in Southern Ontario. Environmental Geotechnics,.

Wolff, T.F. 1994. Evaluating the reliability of existing levees.

Xue, J.F., and Gavin, K. 2007. Simultaneous determination of critical slip surface and reliability index for slopes. Journal of Geotechnical and Geoenvironmental Engineering, **133**(7): 878–886.